Study of Solid-Phase Reactions of metals on GaAs

Boon-Khim Liew

Senior Thesis

Department of Electrical Engineering
California Institute of Technology
Pasadena, California.

June 3, 1985

Acknowlegdements

I wish to express my profound appreciation to my supervisor Prof. M-A. Nicolet for his guidance, encouragement and support, and to Dr. H. P. Kattelus for introducing me to this exciting study of contacts to GaAs from which my thesis topic emerged and also providing me with incessant advice and refinement to all my work.

My gratitute goes to Dr. J. L. Tandon of Applied Solar Corporation, City of Industry, California, who contributed many fruitful discussions and comments as well as assistance in SEM and EDAX analysis.

Many thanks to Frank So, Tom Banwell, Dr. E. Kolawa and Dr. X-A. Zhao for unselfishly offering their help in part of the experimental work and giving many useful suggestions. I am also grateful to Wayne Lam for preparing evaporated back contacts.

I am indebted to Prof. D. Rutledge for giving me access to the Semiconductor Parameter Analyzer and the HP 1MHz C-meter. My appreciation also goes to Ringe Shima and Jack Collier of Jet Propulsion Laboratory, California Institute of Technology, for assistance in SEM and EDAX analysis, Rob Gorris and Concetto Geremia for their technical assistance.

The gift of GaAs wafers for this study by Applied Solar Corporation is gratefully acknowledged.

Last but not least, I wish to pay a special respect to my parents whose confidence and expectation in me are my constant source of spiritual support. It is to them that this work is dedicated.

Abstract

To make stable and reproducible contacts to GaAs, metals which react with GaAs in the solid-phase should be favored. In this study, contacts formed employing Pd/TiN/Pd/Ag, Pd:Mg/TiN/Pd:Mg/Ag and Ru/TiN/Ru/Ag are studied. The TiN layer is included to investigate its application as diffusion barrier in these metallizations. Contacts to n-GaAs are rectifying and the value of barrier height is modified upon annealing. Contacts to p-GaAs are initially rectifying but exhibit ohmic behaviour after annealing. The modifications in the electrical properties are attributed to the solid-phase reaction of metal and GaAs. The integrity of the contacts relies critically on the success of TiN to prevent the intermixing of Ag overlayer and the underlying layers. At elevated annealing temperatures (450°C), TiN fails to function as a diffusion barrier. As a result, the properties of the contact deteriorates.

Table of Contents

	page
Acknowledgements	i
Abstract	ii
Table of Contents	iii
I. Introduction	1
II. Experimental Procedures	5
III. Results and Discussion	
1. Backscattering	9
2. Microscopy and EDAX	11
3. Contact Resistivity	12
4. I-V and C-V Characteristics	14
IV. Conclusion	17
References	19
Table	22
Figures	23

I. Introduction

With the increasing device application of GaAs, much interest has arisen in the study of ohmic and Schottky contacts to GaAs. The contacts are necessary to provide electrical connection between devices and the outside world. Depending on device application, the electrical connection must provide: (a) an ohmic contact with low contact resistivity; or (b) a rectifying (Schottky) contact. In either case, the requirements on the contacts are: thermal stability, lateral uniformity, reproducibility and good adhesion with the underlying substrate and overlaying metal.

The properties of metal-semiconductor Schottky barrier (i.e. its height and width) directly affect the current transport across the interface [1,2]. There are four modes of current transport processes across the metal-semiconductor contact: (a) thermionic emission of carriers over the top of potential barrier; (b) thermionic field emission by tunneling of carriers through the top of barrier; (c) field emission by tunneling of carriers through the whole barrier, which is the preferred mode of current transport in ohmic contacts; (d) recombination in space-charge or neutral regions. The second and third processes are enhanced by doping the semiconductor at the interface to narrow the depletion region.

Although GaAs devices have made steady progress since the 60's, present contact technology is still far from satisfactory. GaAs devices such as Schottky barrier IMPATT diodes, MESFETs and Gunn oscillators place severe requirements on the properties of electrical contacts. A survey of reliability assessments performed by various manufacturers identifies contact degradation as the primary failure mode in these devices [3]. Conventional ohmic contacts to GaAs are fabricated using an eutectic composition of metal and dopant element, such as Au:Ge, Au:Sn, Ag:Ge for contacts to n-type GaAs and Au:Zn, Au:Be, Ag:In for

contacts to p-type GaAs. A small amount of Pt or Ni is usually added to assist wetting during the alloying process. The silver or gold based contacts alloyed in a conventional furnace (e.g. at 440°C 20min for Au:Ge/Ni contacts) suffer from problems associated with reliability, reproducibility and uniformity [4]. Significant interdiffusion of Au and Ga occurs after prolonged heat treatment of such contacts [3]. The Au in-diffuses into the substrate creating spikes which can short a shallow junction, and the Ga dissociates from the substrate and out-diffuses to the Au overlay forming intermetallic phases with high resistivity. Furthermore, since contact formation relies on the alloying reaction at the interface which is highly sensitive to process parameters such as the temperature and time of the alloying cycle, and the amount of materials. As a result, the contact resistivity (ρ_c) is difficult to reproduce. Contacts alloyed using pulsed laser and pulsed electron beam are reported to be superior to those alloyed in furnace [5,6]. The short and controlled alloying cycle produces contacts with improved surface morphology, reproducibility, and contact resistivity (5×10^{-6} Ωcm^2 using pulsed laser [5] and 4×10^{-7} Ωcm^2 using pulsed e-beam [6]) than furnace-annealed contacts. The improved properties are attributed to the small amount of intermixing of Au and the substrate material in laser and e-beam annealing. However, these contacts are still susceptible to degradation after further heat treatment (e.g. at 250°C 500h [7]), suggesting short life time in practical device applications.

Studies have shown that the contact resistivity in Au:Ge/Ni system is directly related to the different phases present at the interface [8]. Low contact resistivity in this system correlates with the presence of the ternary phase Ni_2GeAs. The highly irregular nature of these "good" Ni_2GeAs areas is clearly shown in the cross sectional TEM study performed by Kuan *et al*. The contact resistivity depends on the size and destribution of this phase and is dominated by the spreading resistance of the Ni_2GeAs grains. It is calculated by Braslau to

be inversely proportional to the size and density of the grains [4]. The deterioration of contact resistivity upon further annealing is due to the in-diffusion of Au which reduces the density and relative area of Ni_2GeAs.

In another approach to form contacts to GaAs, an epitaxial layer is formed on the GaAs substrate to create a heterojunction using Ge by MBE [9] or $In_xGa_{1-x}As$ by heat treatment of evaporated In film [10] on GaAs. The resultant heterojunction produces favorable energy band alignment for current conduction. Metal contacts are then made to this epitaxial layer. A contact resistivity of 10^{-6} Ωcm^2 is reported for Au:Mo/Ge-GaAs [9], and 10^{-5} Ωcm^2 for $In/In_xGa_{1-x}As$-GaAs contacts [10]. The reliability of these contacts has yet to be assessed.

Other studies of contacts to GaAs aim at exploiting solid-phase reaction between metal and GaAs. These contacts have substantial advantages over alloy based contacts in terms of uniformity and reproducibility. A desirable scheme for ohmic contacts to GaAs would be to find a transition metal (e.g. Ti, V, Ta, Ru, Mo, Pd, Ni, Pt) that reacts with GaAs, and forms thermally stable compound(s) with low potential barrier for ohmic conduction. Some of the recent studies in this direction use Ti [11], Pt, Pt/Mg [12], Pd/Ge [13]. The contact resistivity values reported in these studies vary from 10^{-2} to 10^{-6} Ωcm^2. The value can be reduced by incorporating a dopant in the metal-semiconductor interface. Other studies have investigated the reactions of Ta, Ni, Cr, Mo, W, Ti, Pd with GaAs [14-18]. However, the solid-phase reaction of metals with GaAs has yet to be fully understood. Information on the kinetics and chemistry of the reaction is needed to characterize the reaction.

In this work, various contact systems using Pd and Ru are investigated. A dopant element is incorporated in the metallization to study the effects of such element in the solid-phase reaction. A TiN layer is interposed between the Ag overlayer and the reacting metal films on the substrate. This layer serves two

purposes: (a) it confines the reaction of the metal film and GaAs; and (b) it prevents intermixing of the reaction products with Ag overlayer. The success of TiN as a diffusion barrier in contacts to Si is well established [19]; it has been found effective also in Ti/TiN/Ag [11] and Pt/TiN/Ag [12] contacts to GaAs.

II. Experimental Procedures

Contacts were made to <100> GaAs substrates. Te-doped n-type substrates were used for Rutherford Backscattering analysis; MOCVD-grown Zn-doped p-type ($N_A \simeq 10^{18}$ cm^{-3}) layers, 0.5μm thick, on <100> n-type GaAs substrates were used for contact resistivity measurement; substrates consisting of an n-type ($N_D \simeq 1.5\times10^{17}$ cm^{-3}) epi-layer, 2μm thick deposited on n^+ ($N_D \simeq 2\times10^{18}$ cm^{-3}) GaAs were used for Schottky barrier and I-V characteristics measurements. The substrates were cleaned in organic solvents (TCE, acetone and methanol) and prior to loading into the sputtering chamber, the surface of GaAs was etched in 1:1 H_2O:HCl for 30s to remove native oxides.

For Schottky barrier height measurement, a sintered AuGeNi contact was first formed on the entire backside of the n/n^+ substrate to provide electrical contact. Au-Ge film, 300Å thick was deposited in vacuum from a preformed eutectic composition (88 wt% Au and 12 wt% Ge). This was followed by the deposition of Ni film about 200Å thick. A final Au evaporation brought the total contact thickness to 3000Å. The sintering was accomplished in flowing H_2 gas at 420 °C for 30s.

The contact on the front surface whose properties are investigated in this study was next applied and consisted of a multilayer structure with a layer of transition metal (Ru, Pd or Pd co-sputtered with Mg), followed by a diffusion barrier layer TiN and then the Ag overlayer. A small amount of the transition metal in contact with GaAs was also deposited on TiN to improve the adhesion of Ag to TiN. The various layers were deposited by RF magnetron sputtering which was performed in vacuum chamber equipped with 7.5cm in diameter planar magnetron cathodes. The target plates all have the nominal purity levels better than 99.99%. In the co-sputtering of Pd:Mg, a thin stripe of Mg, was placed in contact with the Pd target. The chamber was evacuated to a background pressure of

2.0×10^{-6} Torr. Prior to the deposition, the system was backfilled with gas; the composition and pressure are given in table 1 together with other sputtering parameters. Pd, Pd:Mg, Ru and Ag layers were sputtered in Ar ambient. Films of TiN were prepared by reactively sputtered Ti in a pre-mixed gas of 80 mol% Ar and 20 mol% N_2. In Pd, Pd:Mg, Ru and Ag depositions, the substrate table was connected to ground potential, but in TiN deposition, a dc bias of -50V was applied to the subtrate to improve the properties of TiN layer. All the depositions were performed in the dynamic sputtering mode: the substrates cyclically pass beneath the orifice under the target. The rotation speed of the substrate table was about 2RPM. The thicknesses of the films determined by BS measurement are given in figure 1, assuming bulk density values.

The samples were furnace-annealed from 250°C to 550°C in a sequence of 50C° temperature steps and the annealing time was 30 min. The annealing was performed in vacuum 5×10^{-7} Torr up to 400°C. Subsequent thermal annealing was done in an open tube furnace with flowing forming gas (15 mol% H_2, 85 mol% N_2) having a flow rate of $200cm^3/min$. After each annealing step, electrical measurements and RBS spectra were taken.

For contact resistivity measurement, circular contacts (figure 2) conforming to the circular transmission line model (CTLM) were made photolithographically by lift-off on the substrates. The advantage of a circular geometry over the conventional in-line geometry is that only one patterning step is required. Contact resistivity measurements were made by employing four probes; two for current and two for voltage. This method eliminates the contribution of the probe resistance in the measurement. The values of resistance were taken with a HP3456A digital voltmeter, which is capable of 4-wire resistance measurement. The contact resistivity, the sheet resistance of epi-layer outside the contact (R_{sh}) and sheet resistance below the contact (R_{sk}) (see figure 3) were deter-

mined by the method of Reeves [20].

For current-voltage and capacitance-voltage measurements, arrays of circular Schottky diodes were defined by standard lift-off procedures. The measurements were made using a HP Semiconductor Parameter Analyzer. Capacitance values were measured by HP 4280A 1MHz C Meter. The data collected from IV measurements were analyzed by assuming the thermionic emission model to find the barrier height φ_{Bn}^{IV} and ideality factor n [21]:

$$I=AA^{**}T^2\exp\left(\frac{-q\varphi_{Bn}^{IV}}{kT}\right)\exp\left(\frac{qV}{nkT}\right) \quad (1)$$

$$\varphi_{Bn}^{IV}=\frac{kT}{q}\ln\left(\frac{AA^{**}T^2}{I_0}\right) \quad (2)$$

$$n=\frac{q}{kT}\frac{\partial V}{\partial(\ln I)} \quad (3)$$

where I_o is the intercept of the log I vs V plot at V=0 and A^{**} is equal to 8.4 $Acm^{-2}K^{-2}$ for GaAs [22].

The voltage dependence of the barrier capacitance was found in the form of $1/C^2$ vs V plot. According to the one-sided abrupt junction model, the depletion capacitance is related to the reverse bias voltage by:

$$\frac{1}{C^2}=\frac{2}{q\varepsilon\varepsilon_0 N_D}(V_d-V) \quad (4)$$

where ε is the relative dielectric constant of GaAs; ε_0 is the permittivity of free space, N_D is the donor concentration which can be derived from the slope of $1/C^2$ vs V and V_d the built-in voltage equals to the intercept on the voltage axis. The barrier height is given by [21]:

$$\varphi_{Bn}^{CV}=V_d+\frac{kT}{q}\ln\left(\frac{N_C}{N_D}\right)+\frac{kT}{q}-\Delta\varphi_i \quad (5)$$

N_c is the effective density of states in the conduction band ($4.7\times10^{17}cm^{-3}$) [21]. The second term in the equation is the energy difference between the

conduction band edge and the Fermi level. The third term is the correction for thermal energy. $\Delta\varphi_i$ is the image-force lowering of the barrier height and is given by [21]:

$$\Delta\varphi_i = \sqrt{\frac{q}{4\pi\varepsilon\varepsilon_0}\left(\frac{qN_DV_d}{\varepsilon\varepsilon_0}\right)^{\frac{1}{4}}} \tag{6}$$

The depth distribution of the atoms in the contacts was determined by Backscattering measurement. The 2MeV $^4He^+$ beam incidence was normal to the sample and the detector was placed at a scattering angle of 163°.

III. Results and Discussion

1. Backscattering

The interaction of metal(s) with GaAs in the contacts is monitored as a function of annealing temperature by BS measurement. Four spectra for Pd/TiN/Pd/Ag contacts before and after annealings for 30min at 400°C, 450°C and 550°C are shown in figure 4. The spectrum of the as-deposited sample shows sharp edges in the Ag signal, and the Gaussian energy profiles of the Ti and the two Pd layers. The substrate signal has a slanting front edge which indicates some out-diffusion of substrate material. This initial movement of Ga or As might be resulted from the temperature increase during sputtering.

After annealing at 400°C, BS spectrum does not show broadening and height reduction in the Ti signal which would indicate chemical changes in the TiN diffusion barrier. The integrity of the TiN layer is further confirmed by the unchanged "trough" between the two Pd signals separated by the energy loss within TiN. The small Pd step at the trailing edge of Ag signal which is present in the as-deposited sample has disappeared, indicating the reaction of Ag and the first Pd layer. At the Pd/GaAs interface, interdiffusion begins to occur. The signal of the deep Pd layer is reduced in height, and the front edge of the substrate signal moves toward high energies. The lack of sharp edges in the GaAs signal is an indication of a laterally non-uniform reaction between Pd and GaAs. Compounds such as PdGa, Pd_2Ga, $PdAs_2$ are probably formed at this stage. Olowolafe *et al* have identified the formation of $PdAs_2$ as the first phase owing to the fast diffusivity of As compared to Ga in Pd [18]. However, a more stable phase PdGa eventually evolves at high temperatures (450°C) causing the segregation of $PdAs_2$ at the Pd surface [17]. A calculation is performed to find the backscattering energy from As and Ga atoms at the deeper Pd/TiN interface. The results indicate no penetration of Ga or As into the TiN layer.

The BS spectrum of the sample after 450°C annealing shows significant interdiffusion between Pd and GaAs which is an indication of strong reaction. The entire layer of Pd has reacted, as seen by the widening of Pd signal. However, the signals from various elements overlap, making characterization of the reaction products impossible. An indicative feature of the spectrum is the lowering of Ti signal. This together with subsequent EDAX analysis confirms that TiN layer has failed.

The spectrum of 550°C annealed sample shows extensive interdiffusion between the films and the substrate. The height of the Ag signal shrinks, an indication of interaction among Ag, TiN, Pd and GaAs. The contact at this stage has failed completely.

Similar energy profiles are also observed in the BS spectra of Pd:Mg/TiN/Pd:Mg/Ag contacts. The addition of a small amount of Mg in the contacts does not alter the general behavior of the reaction in Pd/TiN/Pd/Ag contacts.

BS spectra of Ru/TiN/Ru/Ag contacts before and after annealing for 30min at 450°C and 550°C are given in figure 5. Comparing the spectra of the as-deposited and 450°C annealed contacts, no interaction is seen in the interfaces, except for some diffusion of Ru into GaAs as indicated by the movement of the trailing edge of the Ru signal. Ru appears to react slower than Pd with GaAs. The diffusion barrier TiN is still intact. The spectrum of 550°C annealed sample shows the onset of reaction, The Ru signal is reduced in height and broadened indicating that the entire layer of Ru has reacted. A plateau can be seen at the front edge of the substrate signal, an indication of the formation of stable compound(s). However, both the slanting edges of the plateau and the Ru signal, suggest a laterally non-uniform character of the reaction. The widening of the Ti signal again confirms the failure of the diffusion barrier. A similar calculation

to find the backscattered energy of As and Ga atoms at the deeper Ru/TiN interface indicates that As and Ga have reached the edge of TiN. The Ru layer deposited on top of TiN is also altered; possibly by the diffusion of Ag or the reaction underneath the layer. The unaltered surface height of Ag signal shows that the underlayer materials (Ga, As, Ru, Ti) have not yet reached the surface of the contact.

2. Microscopy and EDAX

A distinct change in surface morphology is observed in Pd/TiN/Pd/Ag contacts after 450°C annealing. Inspection of these contacts with an optical microscope reveals the appearance of sporadic pits at the surface in comparison to the clean surface of the sample after 400°C annealing. This observation is correlated with the failure of TiN diffusion barrier from BS measurement. SEM micrographs taken for the contacts after annealing at 400°C, 450°C and 550°C are shown in figure 6. The pits are about 4 μm wide and inside the pit is a protrusion of materials from the underlayer. The density of the pits increases with annealing temperature as seen in figure 6(d).

A clear picture of how the barrier fails initially is shown by the little pits that appear in the 550°C annealed sample; the surface is first punctured from underneath and widened into the structure shown in figure 6(d). Energy Dispersive X-rays (EDAX) spectra were taken both from the interior and exterior of the pits (figure 7). The results show that Ga, As, Pd and Ti are more abundant and Ag signal is smaller in the pit than area outside the pit. This clearly indicates a localized failure of TiN barrier. The barrier is apparently still functioning at the area outside the pits.

SEM micrograph of Ru/TiN/Ru/Ag contacts annealed at 550°C does not show the formation of pits at the surface (figure 8). This can be explained by the fact that the failure of the TiN diffusion barrier is less severe at this tempera-

ture in the Ru metallization than in the Pd case, as is also indicated by BS measurement.

3. Contact resistivity

All the as-deposited contacts are found to be non-ohmic. Upon annealing for 30min at 250°C, the Pd/TiN/Pd/Ag and Pd:Mg/TiN/Pd:Mg/Ag contacts become ohmic with contact resistivity $\simeq 1\times10^{-3}$ Ωcm^2 (see figure 12). The values of contact resistivity are found to decrease monotonically for consecutive heat treatments in the temperature range 250-400°C. Its value is 4×10^{-4} Ωcm^2 after 400°C annealing. The decrease in contact resistivity is caused by the progressive reaction of the metal with GaAs. In this temperature range, the values of the sheet resistance underneath the contact (R_{sk}) (see figure 3) differ significantly from the original values, as seen in figure 10, which can be attributed to the reaction at the metal/semiconductor interface. Further annealing of the contacts causes contact resistivity to increase. From the results of BS measurement, this increase of contact resistivity can be correlated with the failure of TiN. A variety of tentative causes can be put forth to explain the increase in contact resistivity: the intermixing of Ag with the underlayer, the modification of electrical properties of TiN layer due to Pd and GaAs reaction, the formation of high resistivity phase(s) in the interaction of Pd and GaAs at 450°C.

The Pd/TiN/Pd/Ag and Pd:Mg/TiN/Pd:Mg/Ag have similar values of contact resistivity and sheet resistance under the contact (R_{sk}) for the temperature range 250-550°C. The modification of sheet resistance under the contact in the Pd:Mg contacts is consistent with the fact that Mg dopes GaAs. The similarity of Pd and Pd:Mg contacts in term of contact resistivity measurements can be explained by slight contamination of Mg in Pd sputtering target after the co-sputtering of Pd:Mg.

The Ru/TiN/Ru/Ag contacts start to exhibit ohmic characteristic after 300°C annealing. Contact resistivity for this annealing temperature is 1×10^{-2} Ωcm^2. The values decrease slightly for the temperature range 300-400°C. After annealing at 450°C, the contact resistivity is reduced by more than a factor of two down to $\times10^{-3}$ Ωcm^2, the result of reaction between Ru and GaAs. Annealing beyond 450°C results in increased values in ρ_c, this again can be attributed to the failure of TiN. An interesting note is that the values of sheet resistance below the contact (R_{sk}) and and the sheet resistance outside the contact (R_{sh}) for Ru contacts are very close, indicating that Ru does not dope GaAs.

The fact that the substrate sheet resistance below the contacts is altered by the reaction warrants consideration in the calculation of the true contact resistivity. Such variation has been taken into account by Reeves' method which involves end resistance measurement. We have performed calculations by assuming the equality of the two sheet resistances. The resultant values of contact resistivity for p-GaAs/Pd:Mg/TiN/Pd:Mg/Ag contacts are found to be about one order of magnitude lower when making the assumption of stable sheet resistance than when considering its modification.

4. I-V and C-V Characteristics

The apparent barrier height from CV measurement φ_{Bn}^{CV} and IV measurement φ_{Bn}^{IV} for contacts to n-GaAs are plotted as a function of annealing temperature in figures 8. The IV barrier height is calculated by extrapolating the thermionic emission current region in the IV characteristics (where the ideality factor $n\simeq1$) (figure 12).

The values of apparent barrier height from CV measurement φ_{Bn}^{CV} found in this work: 1.0V for Pd/n-GaAs and 1.18V for Ru/GaAs are higher than those reported for ideal metal/n-GaAs contacts [27-29]. A large discrepancy between the apparent barrier heights from IV measurement φ_{Bn}^{IV} and CV measurement φ_{Bn}^{CV}

of the as-deposited contacts is observed (see figure 11). The barrier heights measured by CV are higher than those measured by IV technique for both Ru/n-GaAs and Pd/n-GaAs. The difference is 0.6V for the former and 0.4V the latter. This observation and the initial change of the apparent IV and CV barrier barrier heights cannot be explained by the parallel Schottky contacts model [23]. However, it can be accounted for by considering the nonstoichiometric defects at the metal-GaAs interface induced by oxidation and/or metal deposition. Wang *et al* and Amith *et al* have reported divergent IV and CV barrier heights in Au/n-GaAs Schottky contacts with substrate covered by oxide [24,25]. In addition Wang *et al* have shown that magnetron sputtering leads to a higher ideality factor and lower values of apparent IV barrier height φ_{Bn}^{IV} compared to apparent CV barrier height φ_{Bn}^{CV}. Fontaine *et al* in explaining the similarly large discrepancy of measured IV and CV barrier heights in Pt/n-GaAs contacts [26] proposed that these defects (due to oxidation and/or metal deposition), under forward bias might act as recombination centers or intermediate state for trap assisted tunneling. Both current processes have the dependence $\exp(-qV/2kT)$. The result is to increase the ideality factor and decrease the apparent IV barrier height. In the CV measurement, however, since the defects are distributed near the interface, the compensation of these defects causes the $1/C^2$ vs V curve to shift to the left along the voltage axis by ΔV and increases the apparent CV barrier height [26].

$$\Delta V = qN_{ss}d/2\varepsilon_0\varepsilon \qquad \text{(vii)}$$

where N_{ss} is the defect density per unit area and d is the depth of layer containing defects.

The interface defects argument is consistent with the observation that contacts after annealing shows improvement in the ideality factor and better agreement between the values of apparent barrier height from IV and CV meas-

urements. The difference between the measured IV and CV barrier heights diminishes because as the reaction between metal and GaAs proceeds, the interface moves into the bulk region and consumes the defects. At the same time the barrier height is also modified by the metal-GaAs reaction. The values of barrier height for Pd/n-GaAs contacts are 0.78V after annealing at 300°C (These diodes have an ideality factor of 1.2). This is lower than the as-deposited values reported by Waldrop (φ_{Bn}^{CV}=0.93V) [27] and Hökelek *et al* (φ_{Bn}^{IV}=0.87V) [30]. Similarly, the barrier height of Ru/n-GaAs is found to be 0.70V (n=1.1) for contacts after 300°C annealing compared to the as-deposited value φ_{Bn}^{CV}=1.01V reported by Aspnes *et al* [28] (The authors reported the built-in voltage V_d, the barrier height is found from equations (5) & (6)). The lowering of barrier height in these contacts can be explained by the onset of solid-phase reaction which changes the interface chemistry.

After the Pd/n-GaAs contacts are annealed at 350°C, the I-V characteristics develop two main current regions (see figure 12): one due to thermionic emission current I_t and the other due to recombination and/or trap-assisted tunneling current I_r. They can be represented according to the relationships [21]:

$$I_t \propto \exp(\frac{qV}{kT}) \qquad \& \qquad I_r \propto \exp(\frac{qV}{2kT})$$

The sizeable amount of recombination current at low forward voltage is probably caused by the creation of recombination-generation centers as a result of Pd diffusion into GaAs (Olowolafe *et al* have shown that Pd is a fast diffuser in GaAs [18]). In comparison, significant recombination current shows up in the Ru/n-GaAs Schottky diode after 400°C annealing, suggesting that Ru diffusion begins at higher temperature, an observation which is verified by BS measurement.

The forward I-V characteristic of 400°C annealed Pd/n-GaAs contacts (figure 12) shows deviation from the original slopes, indicating that Pd has diffused to the n^+ layer in the substrate causing junction shunting, as is also indicated by the soft breakdown in the reverse characteristics. On the other hand, junction shunting in Ru/n-GaAs contacts occurs after annealing at 450°C. All the devices are shunt out after 550°C annealing as indicated in figure 12. Since junction shunting occurs before TiN starts to fail, the change of barrier height as a result of the diffusion barrier failure can not be determined.

IV. Conclusion

The electrical and metallurgical properties of Pd/TiN/Pd/Ag, Pd:Mg/TiN/Pd:Mg/Ag and Ru/TiN/Ru/Ag contacts on GaAs are investigated in this study. For contacts to p-GaAs, a decrease in contact resistivity is observed with the progressive reaction of metal and GaAs. The lowest value of contact resistivity obtained for Pd/TiN/Pd/Ag contacts is $\sim 4\times10^{-4}$ Ωcm^2 and for Ru/TiN/Ru/Ag contacts $\sim 2\times10^{-3}$ Ωcm^2; these values are obtained after annealing for 30 min at 400°C and 450°C respectively. Because of Mg contamination in Pd sputtering target after the co-sputtering of Pd:Mg, the contact resistivity values for Pd/TiN/Pd/Ag contacts have probably been reduced by the doping effect of Mg.

At elevated annealing temperature, 450°C for Pd/TiN/Pd/Ag and 500°C for Ru/TiN/Ru/Ag contacts, the reaction of Pd or Ru with GaAs is fast and laterally non-uniform. At these temperatures, TiN fails to function as a diffusion barrier. The silver overlayer starts to participate in the reaction of the transition metal and GaAs, resulting in the increase in contact resistivity. The primary cause of the barrier failure is not known, but from BS measurement and SEM microscopy, it is probably due to the non-uniformity and fast kinetics of metal-GaAs reaction which cause TiN diffusion barrier to collapse at localized spots, and hence the formation of pits on the surface. The failure in the Ru/TiN/Ru/Ag contacts is not as severe as in the Pd case. The reaction in the former is slower and starts at higher temperature.

In this study, we have demonstrated that Pd and Ru contacts with an interposed layer of TiN are stable after annealing for 30 min at 400°C and 450°C respectively and have lowest values of contact resistivity at these temperatures. The integrity of the contacts depends critically on the success of TiN layer as a diffusion barrier, when the barrier fails, intermixing of metal overlayer with

materials from the underlayer occurs and the contact resistivity rises. The observation from BS measurement that Ag and Pd in direct contact with each other react at temperatures as low as 300°C underscores the necessity of a diffusion barrier in these contacts.

In addition to contacts to p-GaAs, we have also investigated the electrical characteristics of contacts to n-GaAs. These contacts are rectifying before and after annealing. In both Pd and Ru contacts, a large discrepancy in the IV and CV barrier heights is observed and can be attributed to oxidation and/or sputtering defects. Upon annealing, the values of barrier height are modified by the solid-phase reaction. A large recombination current is observed after annealing at 350°C, which is probably caused by the deep diffusion of metal (Pd or Ru) into the substrate with the creation of traps or recombination centers. Junction shunting occurs in these contacts after annealing at higher temperatures when the metal has penetrated to the n^+ layer in GaAs.

References

[1] A. Piotowska, A. Guivarc'h, and G. Pelous, *Solid-State Electron.* **26** 179(1983).

[2] V. L. Rideout, *Solid-State Electron.* **18** 541(1975).

[3] J. E. Davey and A. Christou in, *Reliability and Degradation* , M. J. Howes and D. V. Morgan, eds. (Wiley, New York, 1981), p.237.

[4] N. Braslau, *J. Vac. Sci. Technol.* **19** 803(1981).

[5] G. Eckhardt in, *Laser and Electron Beam Annealing* , C. W. White and P. S. Percy, eds. (Academic, New York, 1980), p.467.

[6] J. L. Tandon, C. G. Kirkpatrick, B. M. Welch, and P. Fleming in, *Laser and Electron Beam Annealing* , C. W. White and P. S. Percy, eds. (Academic, New York, 1980), p.487.

[7] J. E. E. Baglin, H. B. Harrison, J. L. Tandon, and J. S. Williams in, *Ion Implantation and Beam Processing* , J. S. Williams and J. M. Poate eds. (Academic, Sydney, 1984), p.357.

[8] T. S. Kuan, P. E. Batson, T. N. Jackson, H. Rupprecht, and E. L. Wilkie, *J. Appl. Phys.* **54** 6952(1983).

[9] W. J. Devlin, C. E. C. Wood, R. Stall, and L. F. Eastman, *Solid-State Electron.* **23** 823(1980).

[10] A. A. Lakhani, *J. Appl. Phys.* **56** 1888(1984).

[11] M. F. Zhu, A. H. Hamdi, and M-A. Nicolet, *Thin Solid Films* **119** 5(1984).

[12] H. P. Kattelus, J. L. Tandon, A. H. Hamdi, and M-A. Nicolet, presented at the fall meeting of the Material Research Society, Boston, Mass., Nov. 1984, to be published in the proceedings.

[13] H. P. Grinolds and G. Y. Robinson, *Solid-State Electron.* **23** 973(1980).

[14] A. Lahav and M. Eizenberg, *Appl. Phys. Lett.* **45** 256(1984).

[15] S. D. Mukherjee and C. J. Palmstron, *J. Vac. Sci. Technol.* **17** 904(1980).

[16] O. Wada, S. Yanagisawa, and H. Takanashi, *Appl. Phys. Lett.* **29** 263(1976).

[17] A. Oustry, M. Caumont, A. Escaut, A. Martinez, and B. Toprasertpong, *Thin Solid Films* **79** 251(1981).

[18] J. O. Olowolafe, P. S. Ho, H. J. Hovel, J. E. Lewis, and J. M. Woodall, *J. Appl. Phys.* **50** 955(1979).

[19] M. Wittmer and H. Melchior, *Thin Solid Films* **93** 397(1982).

[20] G. K. Reeves, *A New Technique for the Measurement of Specific Contact Resistance*, Report 7293 Telecom Australia" (1980).

[21] S. M. Sze, *Physics of Semiconductor Devices* (Wiley, New York, 1969).

[22] C. R. Crowell, *Solid-State Electron.* **8** 395(1965).

[23] I. Ohdomari and K. N. Tu, *J. Appl. Phys.* **51** 3735(1980).

[24] Y. X. Wang and P. H. Holloway, *J. Vac. Sci. Technol.* **A 2** 567(1984).

[25] A. Amith and P. Mark, *J. Vac. Sci. Technol.* **15** 1344(1978).

[26] C. Fontaine, T. Okumura, and K. N. Tu, *J. Appl. Phys.* **54** 1404(1983).

[27] J. R. Waldrop, *Appl. Phys. Lett.* **44** 1002(1984).

[28] D. E. Aspnes and A. Heller, *J. Vac. Sci. Technol.* **B 1** 602(1983).

[29] T. Kendelewicz, W. G. Petro, S. H. Pan, M. D. Williams, I. Lindau, and W. E. Spicer, *Appl. Phys. Lett.* **44** 113(1984).

[30] E. Hökelek and G. Y. Robinson, *Solid-State Electron.* **24** 99(1981).

Sputtering Parameters	Deposition				
	Ru	Pd	Pd:Mg	TiN	Ag
Total pressure (in 10^{-3} Torr)	5	5	5	10	5
Gas Composition (in relative partial pressure)	100% Ar	100% Ar	100% Ar	80% Ar 20% N_2	100% Ar
RF power (in W)	500	500	250	800	300
Substrate bias (in V)	0	0	0	-50	0
Deposition time (in min)	3.2	1.3	2.5	10	4

Table 1. Deposition parameters of RF magnetron sputtering.

Figure Captions

Figure 1. Thicknesses of various layers of the contact structure determined from backscattering measurement assuming bulk density values. (a) Pd/TiN/Pd/Ag; (b) Pd:Mg/TiN/Pd:Mg/Ag; and (c) Ru/TiN/Ru/Ag on GaAs.

Figure 2. Contact pattern conforming to Circular Transmission Line Model (CTLM) used for contact resistivity measurement.

Figure 3. The various resistances in the Circular Transmission Line Model. The effect of a modified value of sheet resistance under the contact is taken into account by Reeves' method [20].

Figure 4. Backscattering spectra of four Pd/TiN/Pd/Ag samples before and after annealing at 400°C, 450°C and 550°C for 30 min. The spectrum of 450°C annealed sample shows strong and non-uniform reaction which probably results in the failure of TiN diffusion barrier. The reaction of Ag and first Pd layer has already started at 400°C, as shown by the absence of the small step at the trailing edge of Ag signal.

Figure 5. Backscattering spectra of three Ru/TiN/Ru/Ag samples before and after annealing at 450°C and 550°C for 30 min. The spectrum of 550°C annealed sample shows strong and non-uniform reaction which probably results in the failure of TiN diffusion barrier.

Figure 6. SEM Micrographs of Pd/TiN/Pd/Ag contacts after annealing at (a) 400° (b) 450° and (c) & (d) 550° for 30 min. Pits are seen in the sample after 450°C annealing and their density on the surface increases after annealing at 550°C.

Figure 7. EDAX spectra of Pd/TiN/Pd/Ag contacts after annealing at 550°C for 30 min. The spectra shows Ga, As, Pd and Ti are more abundant but Ag signal is smaller in the pit than area outside the pit, which indicates the

localized failure of the contact. The Al and Fe peaks belong to the background signal of the vacuum chamber.

Figure 8. SEM Micrograph of Ru/TiN/Ru/Ag contacts after annealing at 550°C for 30 min. Pits which would indicate localized failure of TiN diffusion barrier are not found on the surface. The failure of diffusion barrier is not as severe as in Pd/TiN/Pd/Ag contacts.

Figure 9. Contact resistivity (ρ_c) as a function of annealing temperature, 30 min for (a) Pd/TiN/Pd/Ag; (b) Pd:Mg/TiN/Pd:Mg/Ag and (c) Ru/TiN/Ru/Ag contacts on p-GaAs. The values of contact resistivity for all the samples decrease monotonically upon annealing and increase when TiN diffusion barrier begins to fail.

Figure 10. The sheet resistance under the contact (R_{sk}) and the sheet resistance outside the contact (R_{sh}) as a function of annealing temperature, 30 min for (a) Pd/TiN/Pd/Ag; (b) Pd:Mg/TiN/Pd:Mg/Ag; and (c) Ru/TiN/Ru/Ag contacts on p-GaAs. The sheet resistance under the contact for Pd/TiN/Pd/Ag and Pd:Mg/TiN/Pd:Mg/Ag samples is modified by the metal-GaAs reaction. This is due to the doping effect of Mg in the latter contact and slight contamination of Mg in the former one.

Figure 11. The values of ideality factor, barrier height determined from IV (φ_{Bn}^{IV}) and CV (φ_{Bn}^{CV}) measurements as a function of annealing temperature, 30 min for (a) Pd/TiN/Pd/Ag and (b) Ru/TiN/Ru/Ag contacts on n-GaAs. A large discrepancy between values of barrier height from IV and CV measurements is seen for the as-deposited contacts. This discrepancy is attributed to the defects induced by oxidation and/or metal deposition. Better agreement of the two values shows elimination of these defects upon annealing. The values of barrier height for samples after annealing at higher temperatures can not be determined due to junction shunting as a

result of diffusion of Pd or Ru into the n^+ layer in the substrate.

Figure 12. Current as a function of forward voltage for (a) Pd/TiN/Pd/Ag and (b) Ru/TiN/Ru/Ag contacts on n-GaAs after annealing at various temperatures. A significant recombination current is observed after annealing at 350°C for Pd/TiN/Pd/Ag and 400°C for Ru/TiN/Ru/Ag contacts. Junction shunting is seen in both contacts after 550°C annealing when Pd or Ru penetrates to the n^+ layer in the substrate.

Figure 13. $1/C^2$ as a function of reverse voltage for (a) Pd/TiN/Pd/Ag and (b) Ru/TiN/Ru/Ag on n-GaAs contacts before and after annealing at 250°C 30 min. The voltage intercept of the as-deposited curve is shifted to the right on the voltage axis after annealing. This shift is due to the elimination of defects from oxidation and/or metal deposition as well as the modification of barrier height as the metal-GaAs reaction proceeds.

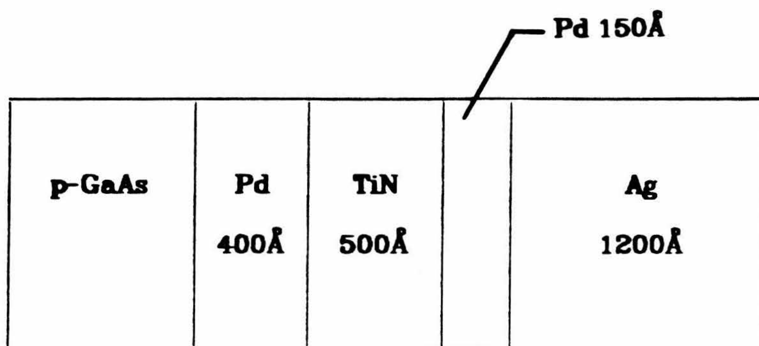

(a)

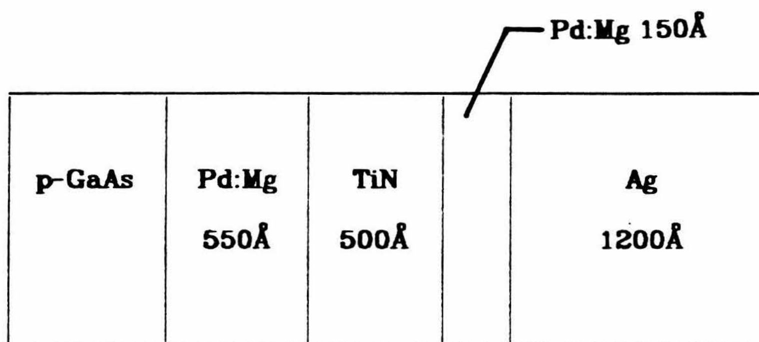

(b)

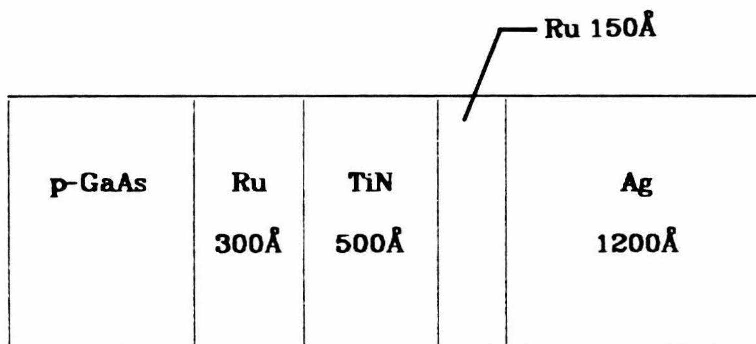

(c)

Figure 1

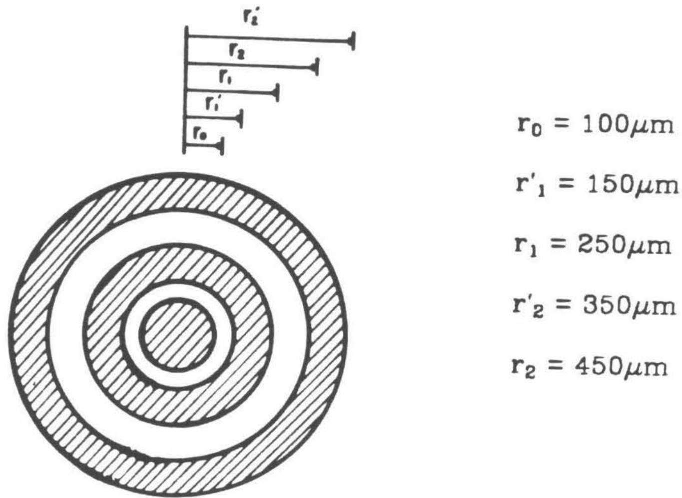

Figure 2

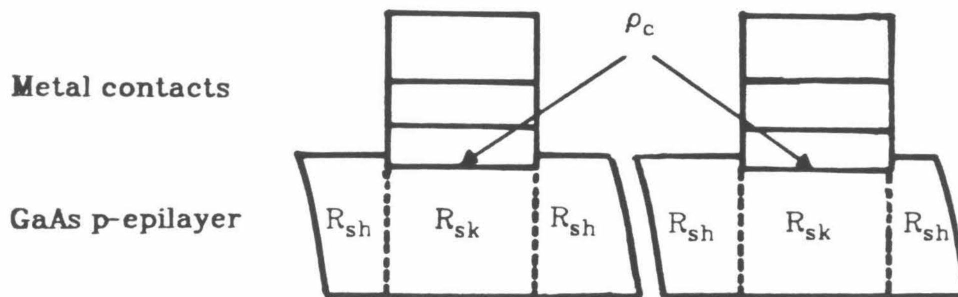

Figure 3

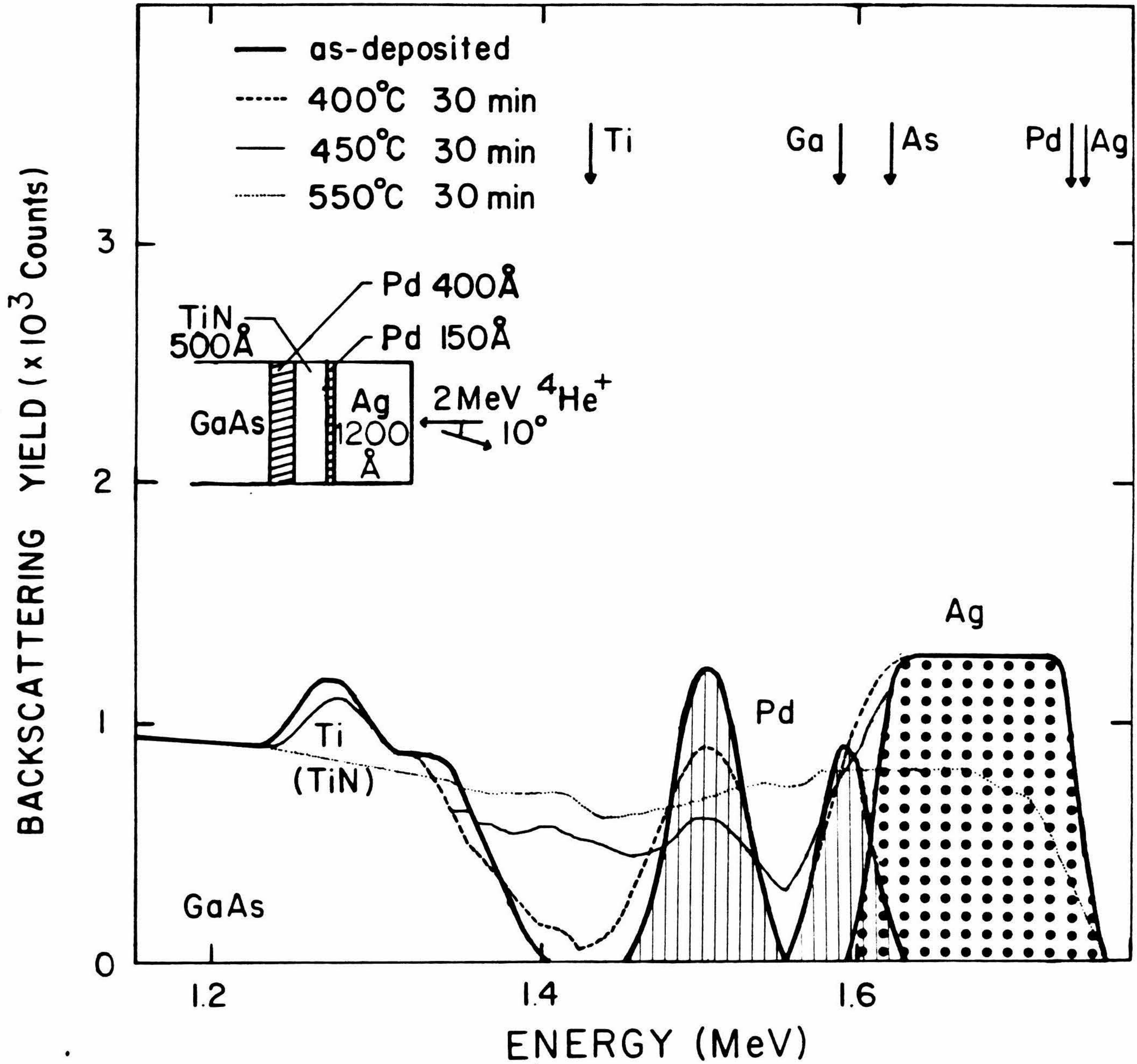

Figure 4

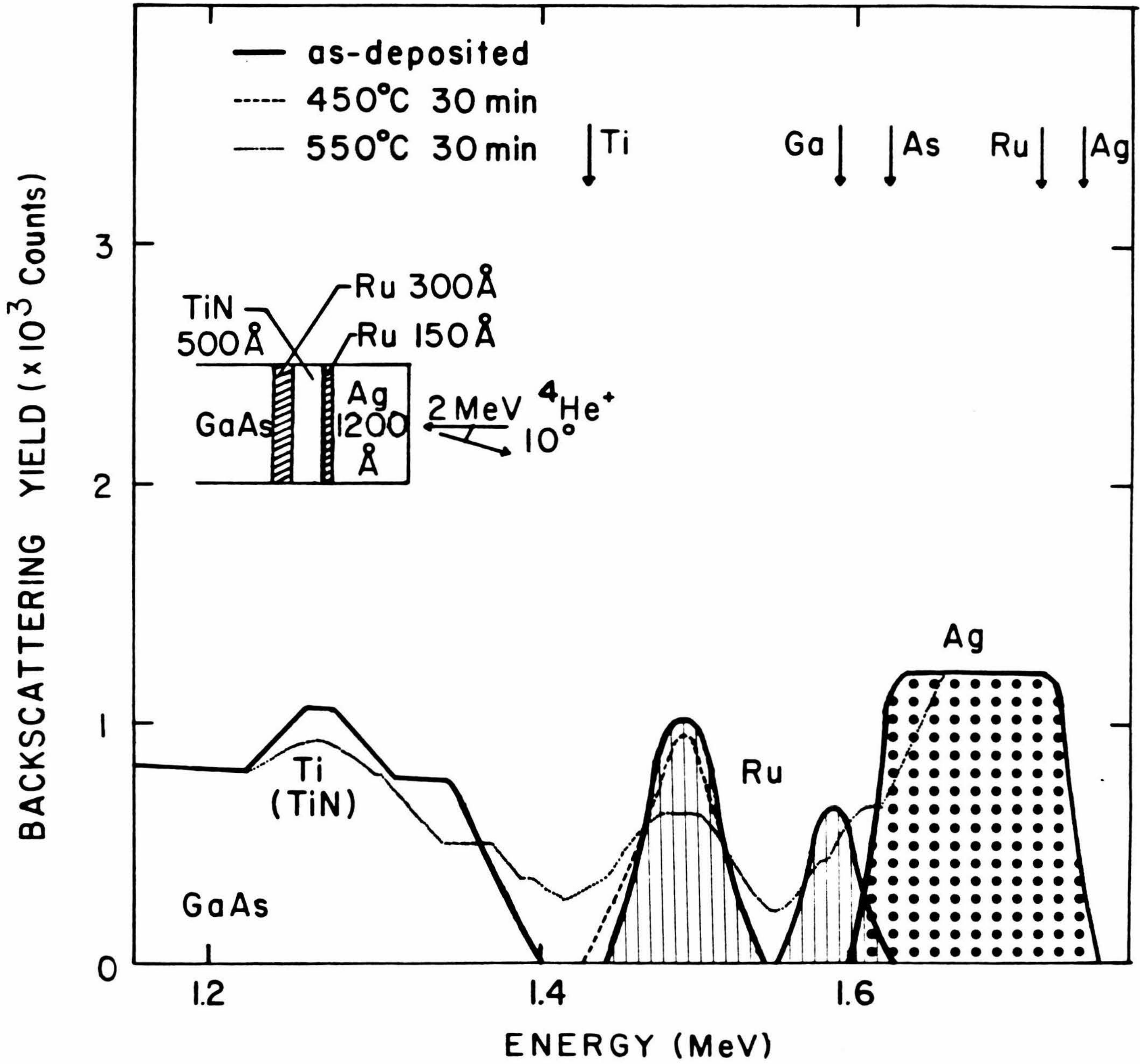

Figure 5.

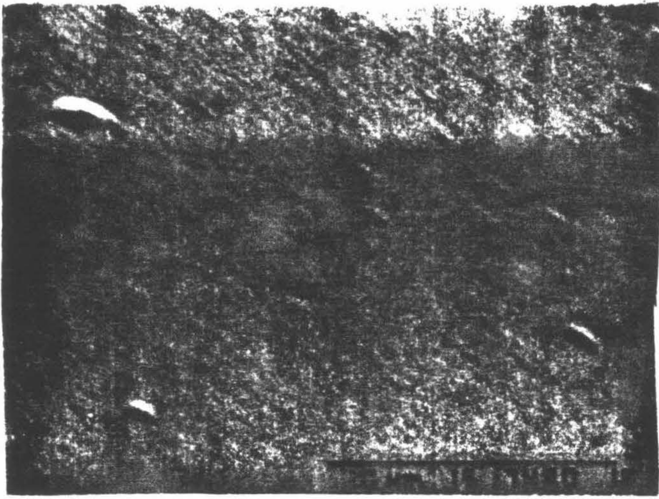

a

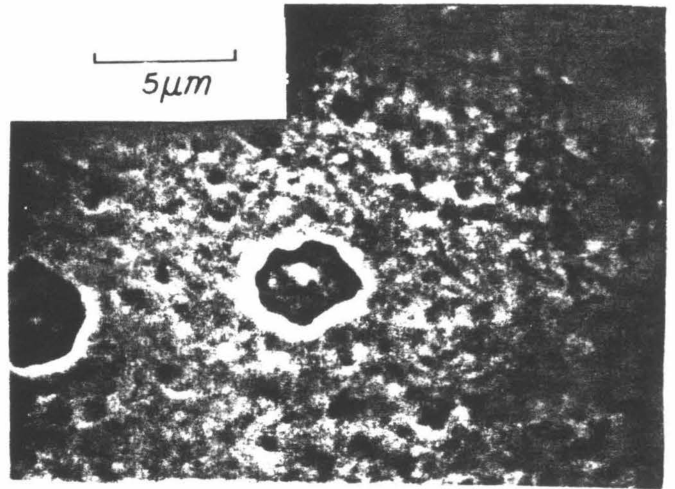

b

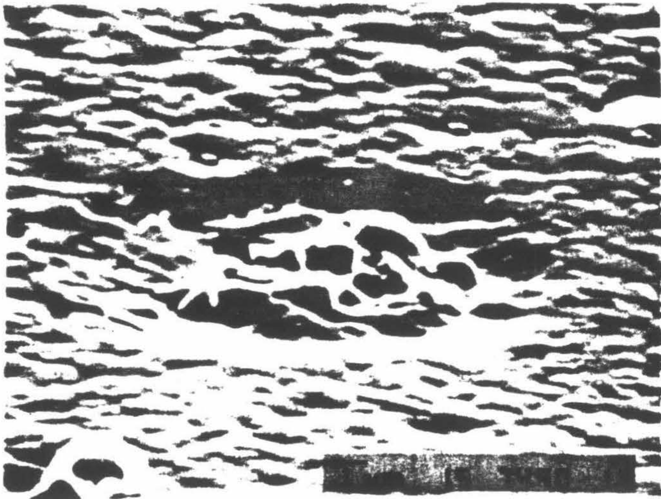

c

d

Figure 6

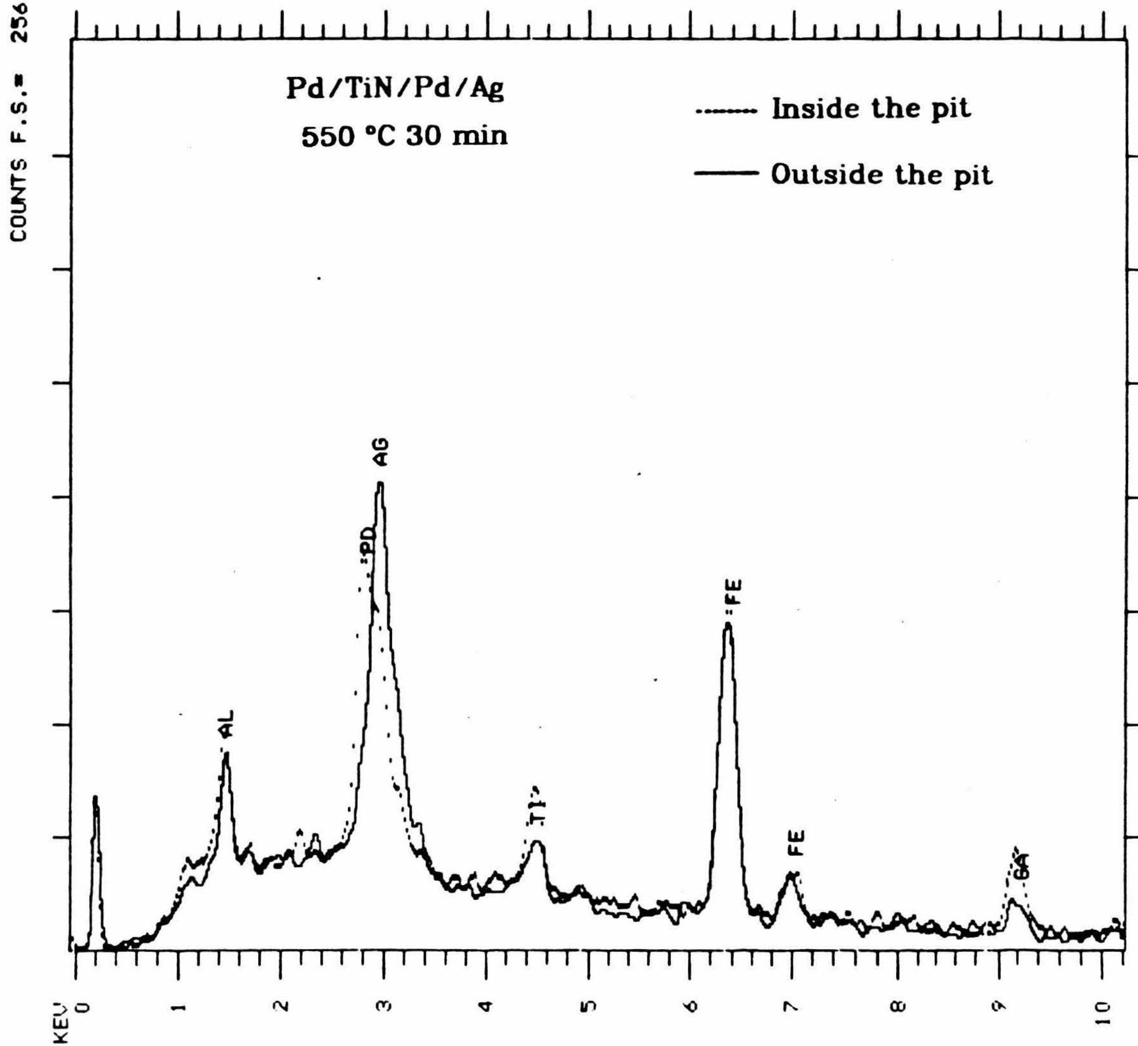

Figure 7

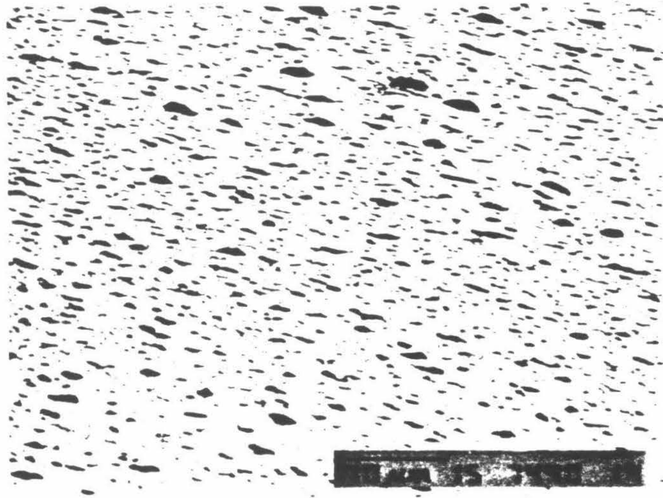

Figure 8

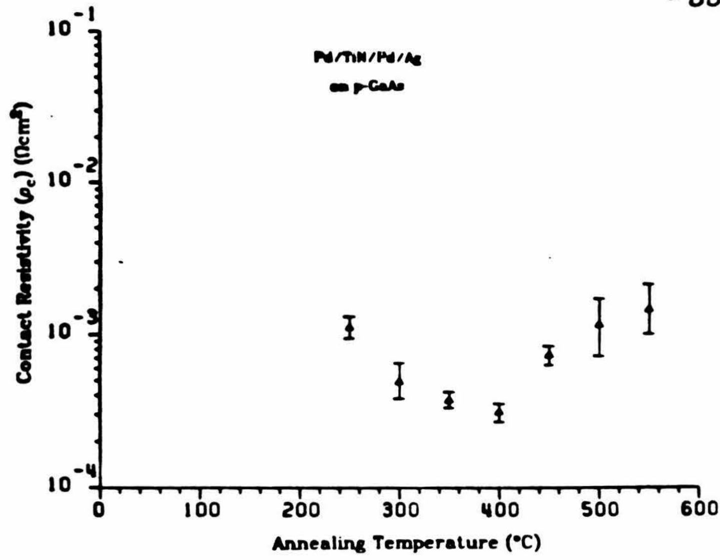

(a)

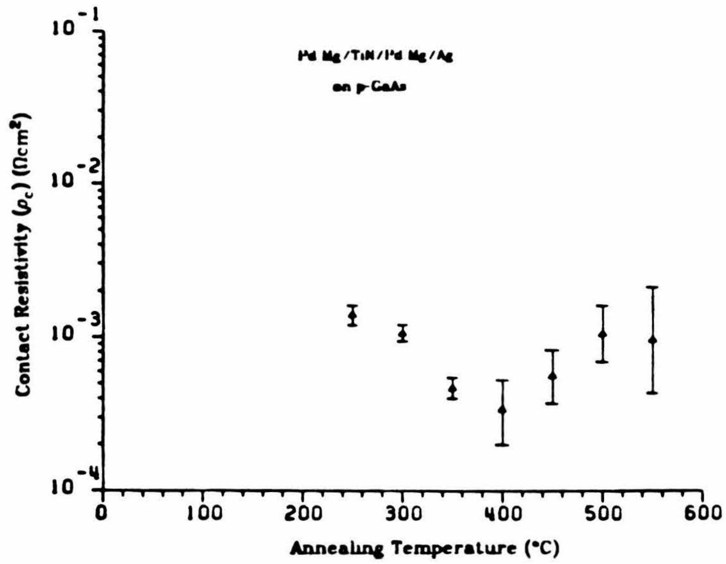

(b)

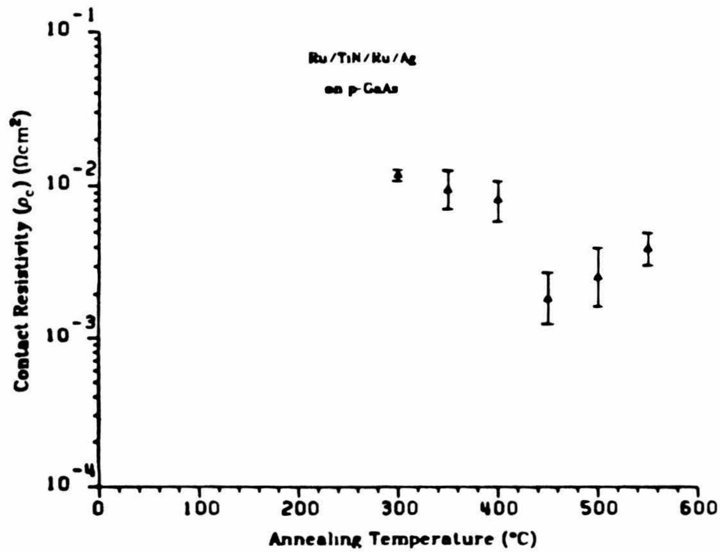

(c)

Figure 9

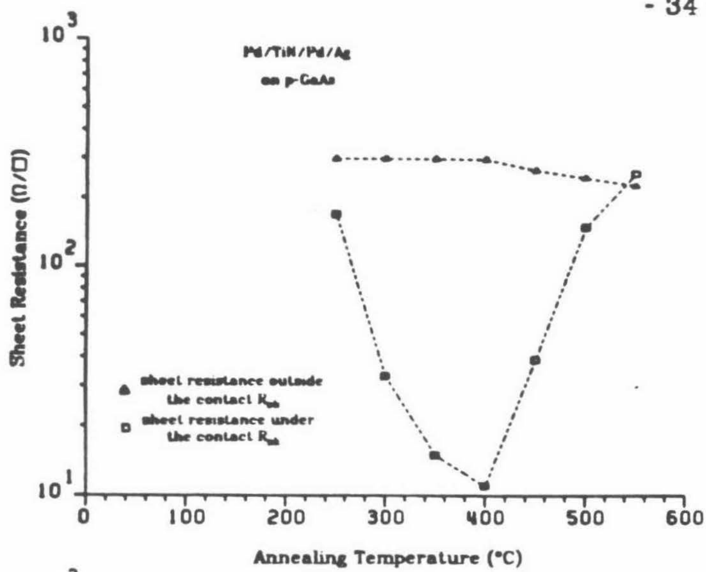

(a)

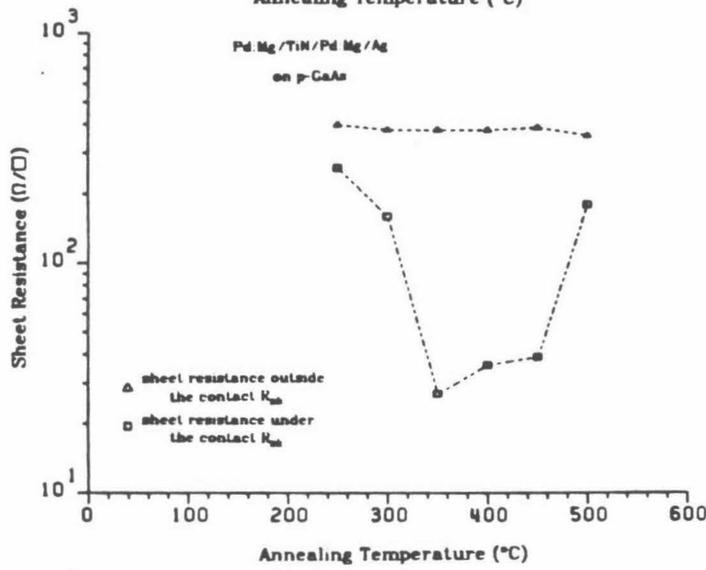

(b)

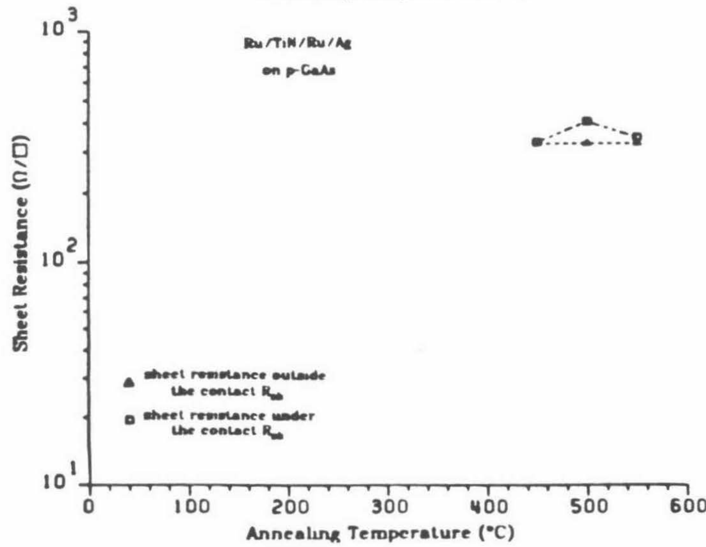

(c)

Figure 10

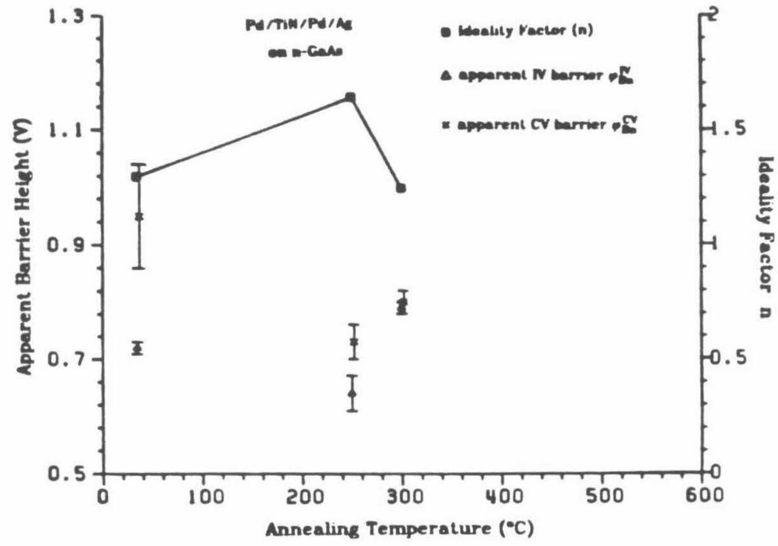

(a)

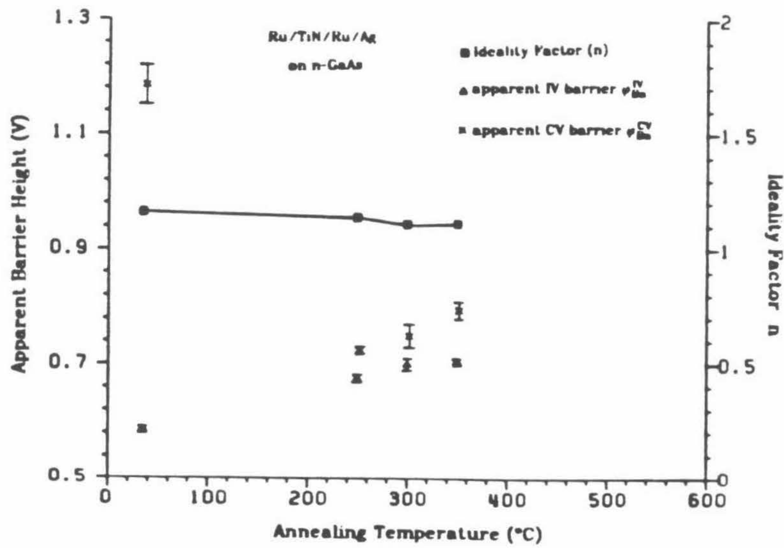

(b)

Figure 11

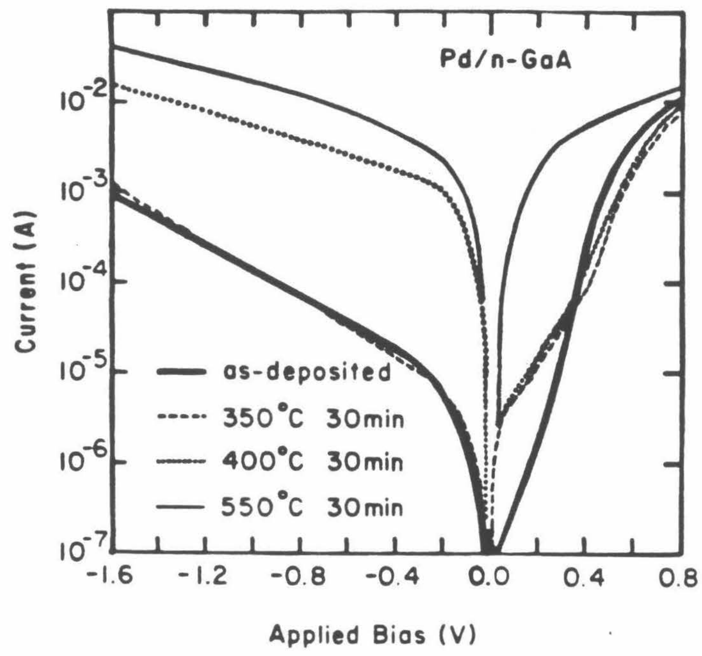

(a)

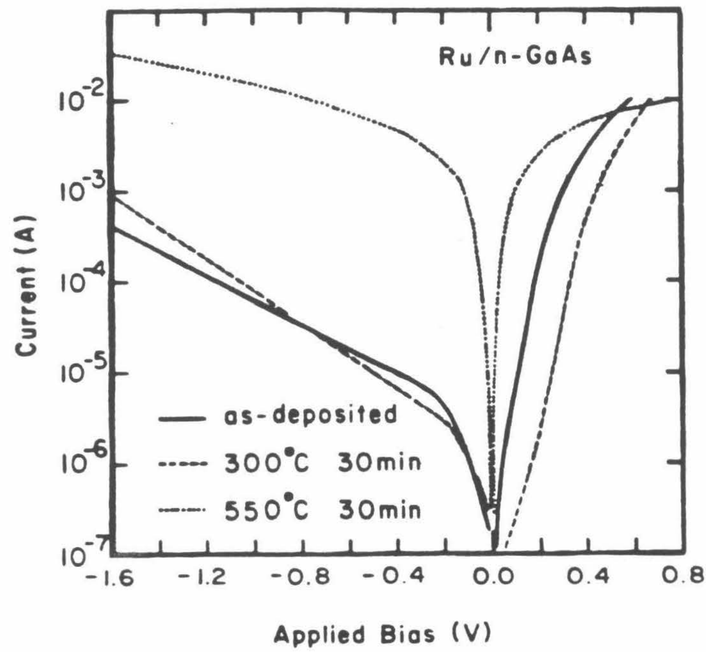

(b)

Figure 12

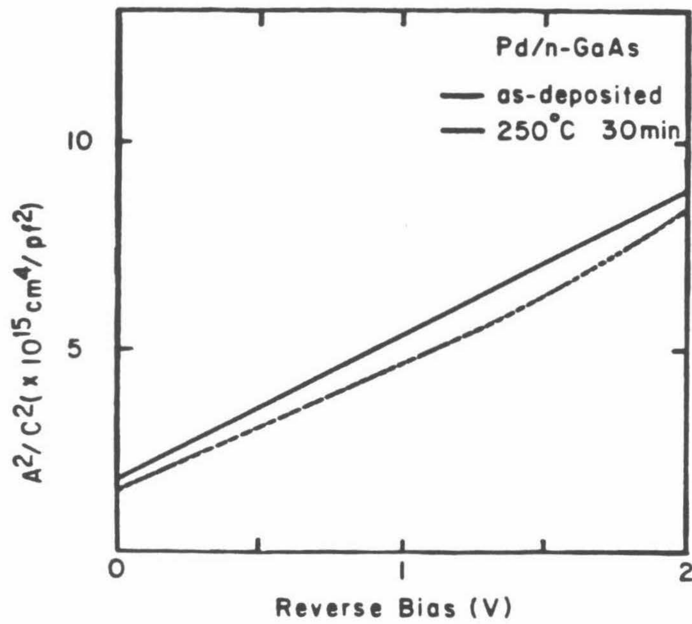

(a)

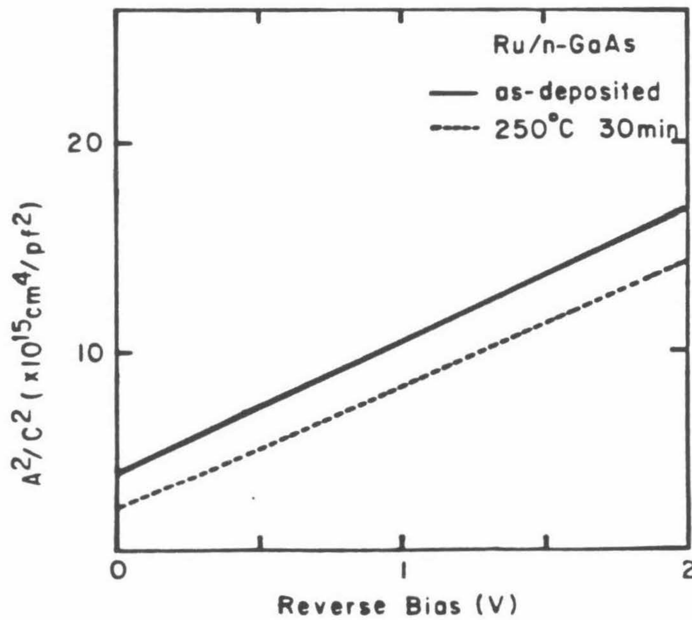

(b)

Figure 13